Physica B 434 (2014) 89–94

Contents lists available at ScienceDirect

Physica B

journal homepage: www.elsevier.com/locate/physb

Dielectric and impedance spectral characteristics of bulk $ZnIn_2Se_4$

M.M. El-Nahass, A.A. Attia, G.F. Salem, H.A.M. Ali*, M.I. Ismail

Physics Department, Faculty of Education, Ain Shams University, Roxy, Cairo 11757, Egypt

ARTICLE INFO

Article history:
Received 2 September 2013
Received in revised form
26 October 2013
Accepted 28 October 2013
Available online 5 November 2013

Keywords:
Dielectric properties
Impedance spectrum
Electrical conductivity

ABSTRACT

The frequency and temperature dependence of ac conductivity, dielectric constant and dielectric loss of $ZnIn_2Se_4$ in a pellet form were investigated in the frequency range of 10^2–10^6 Hz and temperature range of 293–356 K. The behavior of ac conductivity was interpreted by the correlated barrier hopping (CBH) model. Temperature dependence of ac conductivity indicates that ac conduction is a thermally activated process. The density of localized states $N(E_F)$ and ac activation energy were estimated for various frequencies. Dielectric constant and dielectric loss showed a decrease with increasing frequency and an increase with increasing in temperature. The frequency dependence of real and imaginary parts of the complex impedance was investigated. The relaxation time decreases with the increase in temperature. The impedance spectrum exhibits the appearance of the single semicircular arc. The radius of semicircular arcs decreases with increasing temperature which suggests a mechanism of temperature-dependent on relaxation.

1. Introduction

The ternary semiconductor compounds, $A^{II}B_2^{III}C_4^{VI}$, have been widely investigated because of their potential applications to electro-optic, optoelectronic, and nonlinear optical devices. Most of these compounds have defect-chalcopyrites or defect stannite structure [1]. Among them, $ZnIn_2Se_4$, which has potential applications in various fields such as a buffer layer in the fabrication of heterojuction solar cells [2], photoelectronics [3] and electro-optical memory devices [4].

The preparation of $ZnIn_2Se_4$ with a defective chalcopyrite structure has attracted much attention both for fundamental and for applying research [5]. $ZnIn_2Se_4$ material has been prepared by co-evaporation [6,7], chemical vapor deposition [8], spray pyrolysis [9,10], and vertical Bridgman techniques [11]. Bulk $ZnIn_2Se_4$ behaves as p-type semiconductor and it exhibits a change in the sign of the thermo-electric power in the temperature range 90–120 °C. Determination of conduction mechanisms and other electrical properties is believed to be useful in improving stability characteristics of devices based on $ZnIn_2Se_4$ [12]. To our knowledge, there are no reports available on the ac and dielectrical properties of $ZnIn_2Se_4$ in the bulk form.

In the present work, the dielectric and complex impedance spectroscopic properties are reported for $ZnIn_2Se_4$ in the bulk form in the frequency range (10^2–10^6 Hz) and temperature range (293–356 K). Also, the conduction mechanism in the $ZnIn_2Se_4$ is investigated.

2. Experimental technique

Ingots of $ZnIn_2Se_4$ were prepared by fusion of stoichiometric quantities of pure elements in vacuum sealed silica tubes, which were left at 1323 K for 10 h and then cooled to room temperature over 48 h. X-ray diffraction (XRD) pattern was obtained for the powder form using a Philips X-ray diffractometer with Cu(k_α) radiation (λ=1.5418 Å).The powder of $ZnIn_2Se_4$ was thoroughly ground in a mortar to obtain very fine particles, and then it was compressed under a pressure of about 2×10^8 N m^{-2} to obtain a compressed pellet. The resulting pellet has a thickness of 1.33 mm and a diameter of 1.36×10^{-2} m. The two surfaces of the pellet were coated with an evaporated gold film (Au) to serve as Ohmic electrodes. Dielectric and impedance measurements were carried out using a programmable automatic RLC bridge (model Hioki 3532 Hitester). The capacitance and impedance were directly measured in the frequency range 10^2–10^6 Hz. The dielectric constant (ε_1) was calculated using the relation: $\varepsilon_1=Cd/\varepsilon_o A_o$, where C is the capacitance, d is the thickness, A_o is the cross-sectional area of the pellet and ε_o is the permittivity of free space. Also, the dielectric loss (ε_2) was calculated according to the relation: $\varepsilon_2=\varepsilon_1 \tan\delta$, where $\delta=90-\varphi$ where φ is the phase angle. The ac conductivity of the sample (σ_{ac}) was determined from dielectric parameters using the relation: $\sigma_{ac}=\omega\varepsilon_o\varepsilon_2$ [13,14], where ω is the angular frequency. The temperature of $ZnIn_2Se_4$ pellet was measured using a NiCr–NiAl thermocouple connected to the temperature controller over temperature range 293–356 K.

* Corresponding author. Tel.: +20 122906 8680.
E-mail address: hend2061@yahoo.com (H.A.M. Ali).

0921-4526/$ - see front matter © 2013 Elsevier B.V. All rights reserved.
http://dx.doi.org/10.1016/j.physb.2013.10.049

3. Results and discussion

The XRD pattern of $ZnIn_2Se_4$ in powder form is shown in Fig. 1. The diffraction pattern shows that the powder of $ZnIn_2Se_4$ is polycrystalline. The indexing of the reflections with Miller indices has been performed in accordance with Ref. [15], which also shows that has the tetragonal crystal structure with lattice parameters $a=5.5952$ Å and $c=11.9886$ Å [15].

3.1. AC conductivity

Fig. 2 presents the dependence of the ac conductivity (σ_{ac}) on the frequency (10^2–10^6 Hz) of $ZnIn_2Se_4$ pellet at different constant temperatures (293–356 K) on ln–ln plotting. The ac conductivity increases with the increase of frequency, where $\sigma_{ac}(\omega)$ increases gradually for all the temperatures at low frequency then it increases rapidly with increasing frequency. Similar behavior is observed in several semiconductor materials [16–18]. The relation between the ac conductivity and the frequency of the applied field is described by the following equation [19,20]:

$$\sigma_{ac}(\omega) = A\omega^s \quad (1)$$

where A is a constant, ω is the angular frequency and s is the frequency exponent. The exponent s is a very important parameter since its value and behavior with temperature and/or frequency determines the dominant conduction mechanism. According to the quantum mechanical tunneling (QMT) model [21] for the case of non polaron forming carriers, s is predicted to be temperature independent but frequency dependent. For the case of small polaron tunneling, s is predicted to increase as temperature increases. In large polaron tunneling, s should be both temperature and frequency dependent, for small values of polaron radius, s exhibits a minimum at a certain temperature and subsequently increases with increasing temperature in the same way as the case of small polaron QMT. The correlated barrier hopping CBH model [22,23] predicts s to be both temperature and frequency dependent and s should decrease with increasing temperature.

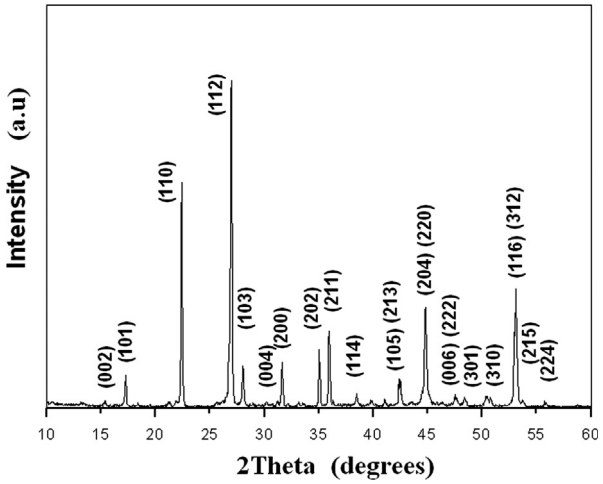

Fig. 1. XRD pattern of $ZnIn_2Se_4$ in the powder form.

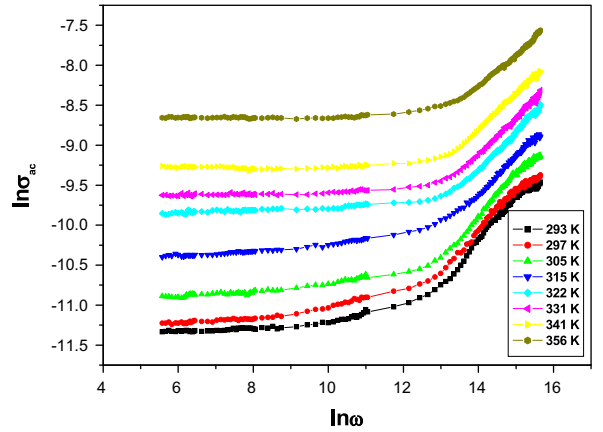

Fig. 2. Frequency dependence of $\sigma_{ac}(\omega)$ of bulk $ZnIn_2Se_4$ at different temperatures.

The value of s for $ZnIn_2Se_4$ at various temperatures is determined from the linear slope of the curves of ln $\sigma_{ac}(\omega)$ versus ln ω. It is noticed that s value decreases with the increase of temperature as shown in Fig. 3. Such a temperature dependence of s and its range of values, for $ZnIn_2Se_4$, are consistent with the correlated barrier hopping (CBH) model.

According to Austin–Mott formula [21], based on CBH model, $\sigma_{ac}(\omega)$ can be explained in terms of hopping of electrons between pairs of localized states at the Fermi level. The process of hopping of electrons is affected also by the density of localized states $N(E_F)$ near the Fermi level. Thus the ac conductivity can be expressed as follows:

$$\sigma_{ac}(\omega) = (\pi/3)[N(E_F)]^2 k_B T e^2 \alpha^{-5} \omega[\ln(\nu_p/\omega)]^4 \quad (2)$$

where k_B is the Boltzmann's constant, e is the electronic charge, α is the exponential decay parameter of localized states wave functions and ν_p is the frequency of the phonons. By assuming $\nu_p = 10^{12}$ Hz and $\alpha^{-1} = 10$ Å [24], $N(E_F)$ was calculated at different frequencies and tabulated in Table 1. It can be observed that the values of $N(E_F)$ decrease with the increase in the frequency.

The variation of ac conductivity with temperature for $ZnIn_2Se_4$ at different frequencies is shown in Fig. 4. The figure shows a semiconductor behavior in the full range of temperature with a linear relationship between lnσ_{ac} and the inverse of temperature at different frequencies. The increase in conductivity with the rise in temperature is due to the increase in the thermally activated electron drift velocity of charge carriers according to the hopping conduction mechanism. The activation energy ΔE_{ac} of the ac conduction is calculated at different frequencies using the well-known Arrhenius equation:

$$\sigma_{ac} = \sigma_o \exp(-\Delta E_{ac}/k_B T) \quad (3)$$

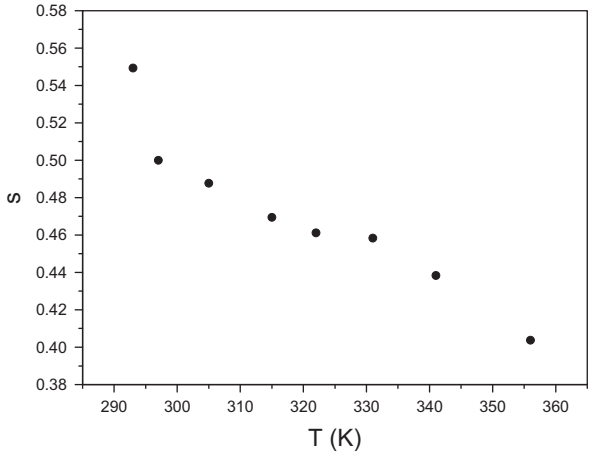

Fig. 3. The variation of the frequency exponent, s with temperature.

Table 1
Values of density of localized states, $N(E_F)$, for bulk $ZnIn_2Se_4$ at different frequencies.

f (kHz)	5	10	50	150	300	600
$N(E_F)$ (10^{23} eV^{-1} cm^{-3})	22.78	18.65	11.00	9.586	9.159	8.216

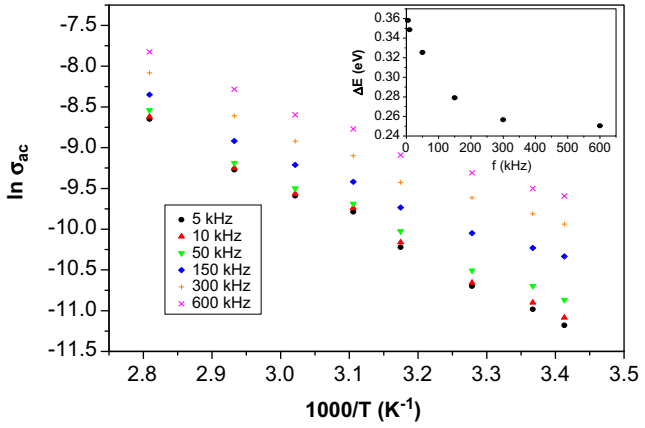

Fig. 4. Temperature dependence of $\sigma_{ac}(\omega)$ of bulk $ZnIn_2Se_4$ at different frequencies; the inset figure represents the variation of ac activation energy (ΔE_{ac}) with temperature.

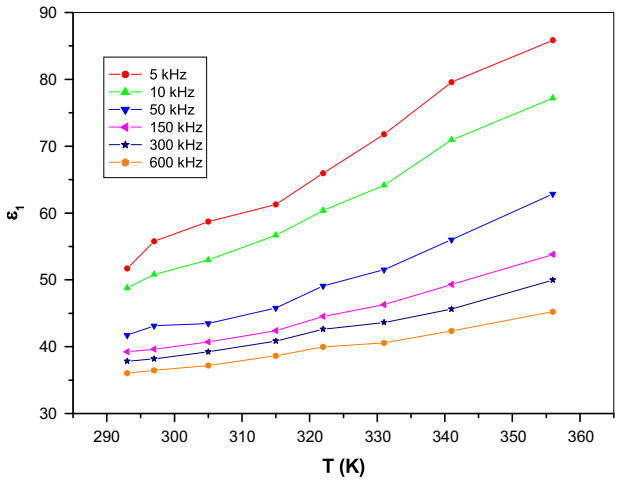

Fig. 6. Temperature dependence of dielectric constant (ε_1) of bulk $ZnIn_2Se_4$ at different frequencies.

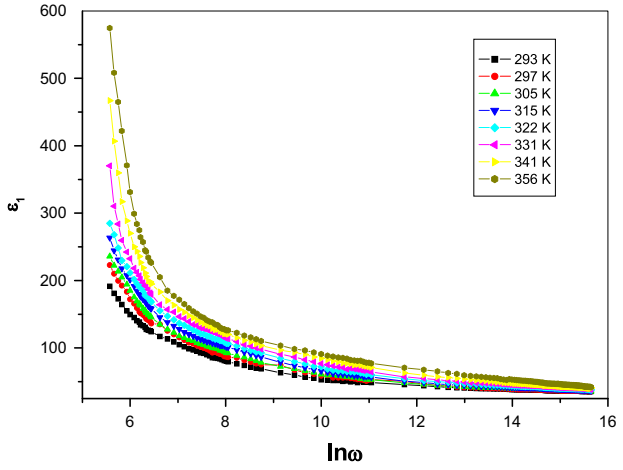

Fig. 5. Frequency dependence of dielectric constant (ε_1) of bulk $ZnIn_2Se_4$ at different temperatures.

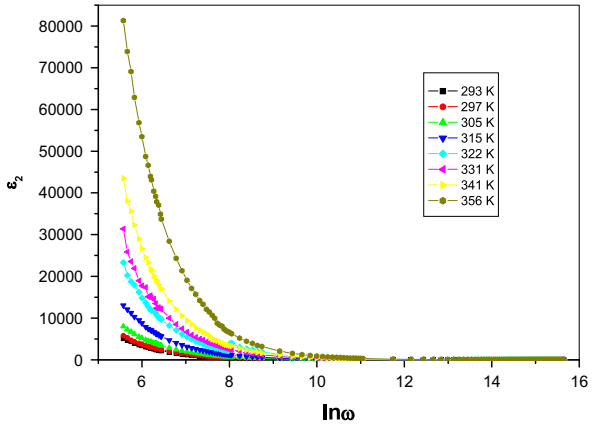

Fig. 7. Frequency dependence of dielectric constant (ε_2) of bulk $ZnIn_2Se_4$ at different temperatures.

where σ_o is a pre-exponential constant. The frequency dependence of ac activation energy for $ZnIn_2Se_4$ is shown in the inset of Fig. 4. It is observed that ΔE_{ac} decreases with increasing frequency. Such a decrease confirms that hopping conduction is the dominant mechanism [25].

3.2. Dielectric constant, ε_1

Fig. 5 illustrates the frequency dependence of the dielectric constant (ε_1) for $ZnIn_2Se_4$ at different constant temperatures. It is clear from the figure that ε_1 decreases with increasing frequency. The observed decrease of ε_1 with the frequency is greater at lower frequency, which can be attributed to the fact that the value of ε_1, at low frequencies, for polar materials is due to the contribution of multicomponent of polarization mechanisms (electronic, Ionic, orientation and interface) [26]. When the frequency is increased the dipoles cannot rotate sufficiently rapidly, so that their oscillations lag behind those of the field. As the frequency is further raised the dipole will be completely unable to follow the field and the orientation polarization ceases, so ε_1 decreases approaching a constant value at high frequencies due to the interfacial polarization only. Fig. 6 shows the temperature dependence of the dielectric constant ε_1 at different frequencies for $ZnIn_2Se_4$. It is clear from the figure that ε_1 increases as the temperature increases over the whole investigated range of frequency. The increase of ε_1 with temperature can be attributed to the fact that dipoles in polar materials cannot orient themselves at low temperatures. When the temperature is raised, the orientation of the dipoles is facilitated and thus increases the orientational polarization, and in turn increases ε_1.

3.3. Dielectric loss, ε_2

Fig. 7 shows the frequency dependence of dielectric loss, (ε_2) for $ZnIn_2Se_4$ at different temperatures. It can be seen that ε_2 decreases with increasing frequency. The decrease of ε_2 with the increase in frequency can be attributed to the fact that the value of ε_2, at low frequencies, is due to the migration of ions in the material. At moderate frequencies ε_2 is due to the contribution of ions jump, conduction loss of ions migration, and ions polarization loss. At high frequency ion vibrations may be the only source of dielectric loss and so ε_2 has the minimum value.

An analysis of the data obtained for the frequency dependence of dielectric loss shows that ε_2 follows a power law with angular frequency as Ref. [27]:

$$\varepsilon_2 = B\omega^m \tag{4}$$

where B is a constant and m is the frequency power factor. Fig. 8(a) represents the relation between ln ε_2 versus lnω for $ZnIn_2Se_4$, which is found to be straight lines at different temperatures. The

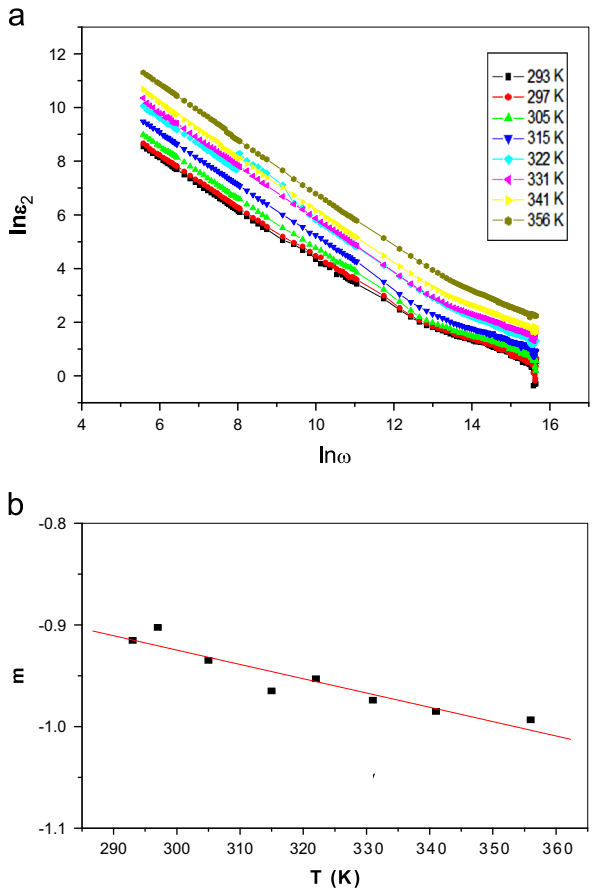

Fig. 8. (a) Plot of ln ε_2 versus ln ω of bulk $ZnIn_2Se_4$ at different temperatures and (b) the variation of parameter m with temperature.

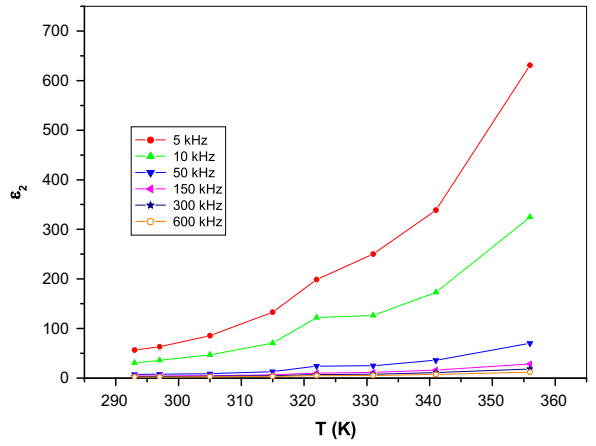

Fig. 9. Temperature dependence of dielectric constant, ε_2 of bulk $ZnIn_2Se_4$ at different frequencies.

values of the power m were calculated from the slopes of the obtained straight lines and represented in Fig. 8(b) as a function of temperature. It can be seen that m tends to decrease with increasing temperature. According to Giuntini model for dielectric relaxation [28]: $m=-4k_BT/W_m$, where W_m is the maximum barrier height. Value of W_m was calculated from the slope of the linear variation of m versus T and was found to be 0.25 eV.

Fig. 9 shows the temperature dependence of dielectric loss of $ZnIn_2Se_4$ at different frequencies. The increase of ε_2 with temperature can be explained by Stevels and Fouad et al. [29,30] who divided the relaxation phenomena into three parts, conduction loss, dipole loss and vibrational loss. At low temperatures, the conduction loss has a minimum value since it is proportional to (σ/ω). As the temperature increases, σ increases and so the conduction loss increases. This increases the value of ε_2 with increasing temperature.

3.4. Complex impedance analysis

The complex impedance spectroscopy is an important tool to analyze the electrical properties and to get more information about the relaxation process of the investigated device [31]. The complex impedance $Z^*(\omega)$ of the investigated material can be described by the following equation [32]:

$$Z^*(\omega)=Z'(\omega)-jZ''(\omega) \quad (5)$$

where Z' and Z'' are ascribed to real and imaginary parts of the complex impedance, respectively. Fig. 10(a) shows the dependence of the real part of the impedance (Z') on the frequency at various temperatures. It is observed that Z' decreases as temperature increases, indicating a negative temperature coefficient of the resistance in the system [33]. The decrease of Z' is up to a certain frequency and then it remains almost constant value with the increase in frequency. The dependence of the imaginary part of the impedance (Z'') on the frequency at various temperatures is shown in Fig. 10(b). It can be seen from the figure that the Z'' spectrum reveals a peak at the different temperatures. The increase of the applied frequency shifts the peak position of towards the high frequency values at different temperatures whereas the increase of temperature decreases the value of the peak.

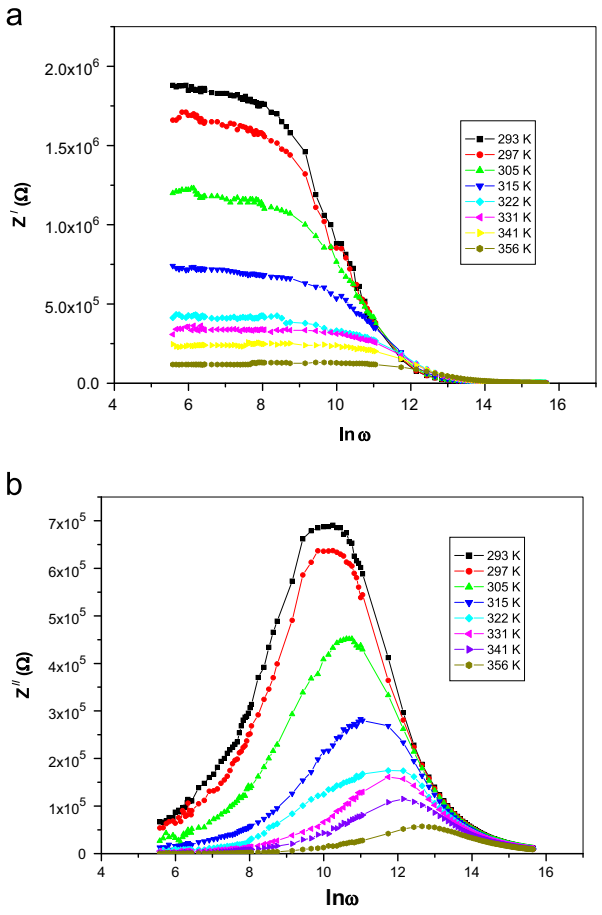

Fig. 10. Frequency dependence of (a) real part, Z' and (b) imaginary part, Z'' of complex impedance of bulk $ZnIn_2Se_4$ at different temperatures.

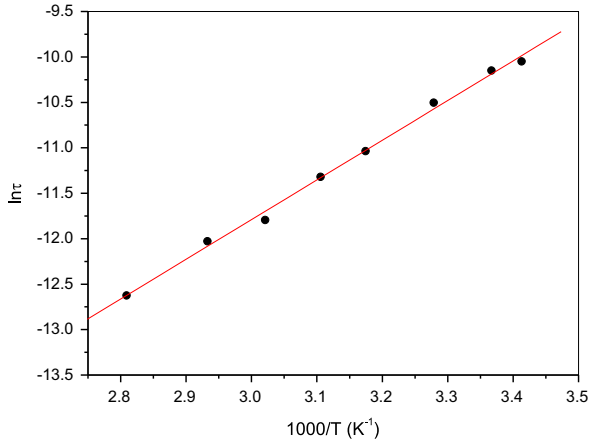

Fig. 11. Plot of ln τ versus 1000/T.

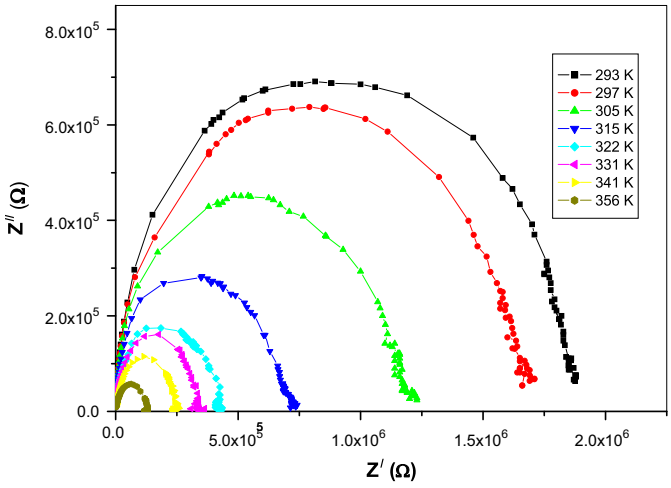

Fig. 12. Complex impedance spectrum (Z'' versus Z') of bulk $ZnIn_2Se_4$ at different temperatures.

The asymmetric peak suggests a spread of the relaxation time (i.e., the existence of a temperature dependent electrical relaxation phenomenon in the material). The relaxation process in the material may be due to the presence of immobile species/electrons at low temperatures and defects/vacancies at high temperatures. In the relaxation system, one can determine the most probable relaxation time (τ) from the position of the loss peak in the Z'' with frequency plots according to the relation: $\tau = 1/\omega$. The ln τ values of $ZnIn_2Se_4$ were plotted as a function of reciprocal temperature $1/T$, as shown in Fig. 11. It is noticed that the relaxation time decreases with the increase of temperature. The experimental data are well described by the Arrhenius expression type, which is given as follows:

$$\tau = \tau_o \exp(\Delta E_a / k_B T) \quad (6)$$

where τ_o is the pre-exponential factor and ΔE_a is the activation energy for the conductivity relaxation. The value of ΔE_a was calculated from the slope of ln τ versus 1000/T plot and it was found to be 0.377 eV.

Fig. 12 shows the complex impedance spectrum (Nyquists diagram, i.e, Z'' versus Z') of $ZnIn_2Se_4$ at different temperatures. It is observed that single semicircular arcs appear at different temperatures. The radius of curvature decreases with increasing temperature which suggests a mechanism of temperature-dependent on relaxation. This single semicircular arc suggests the presence of grain interior (bulk) property of the investigated material [34]. Single semicircular arcs of the impedance spectrum can be modeled as an equivalent circuit consisting of a parallel combination of bulk resistance and capacitance [35]. The values of bulk resistance (R_b) at different temperatures were obtained from the intercept of the semicircular arcs on the real axis (Z') and listed in Table 2. It is noticed that the value of R_b decreases with the increase of temperature.

Table 2
Variation of the bulk resistance, R_b, of $ZnIn_2Se_4$ with temperature.

T (K)	293	297	305	315	322	331	341	356
R_b (MΩ)	1.89	1.70	1.21	0.73	0.44	0.34	0.25	0.13

4. Conclusions

The frequency and temperature dependence of the ac conductivity, dielectric constant, dielectric loss, and complex impedance of bulk $ZnIn_2Se_4$ in a pellet form were investigated in the frequency range of 10^2–10^6 Hz and temperature range of 293–356 K. The ac conductivity increases with the increases in frequency. $\sigma_{ac}(\omega)$ was explained in terms of the correlated barrier hopping (CBH) model. The values of density of localized states, $N(E_F)$, decrease with the increase in the frequency. The ac conductivity is thermally activated process. The activation energy ΔE_{ac} of ac conduction decreases with increasing frequency. The dielectric constant (ε_1) decreases with increasing frequency while increases as the temperature increases. The frequency dependence of dielectric loss shows that ε_2 follows a power law as $\varepsilon_2 = B\omega^m$. While the temperature dependence of the dielectric loss (ε_2) is associated with the conduction loss. The real part of complex impedance (Z') decreases as temperature increases, indicating a negative temperature coefficient of the resistance in the system. The spectrum of the imaginary part of the complex impedance (Z'') reveals a peak at the different temperatures. The asymmetric peak suggests a spread of the relaxation time. The relaxation time decrease with the increase of temperature. Nyquists diagrams of Z'' versus Z' exhibits semicircular arcs at different temperatures. Single semicircular arcs of Nyquists diagram can be modeled as an equivalent circuit consisting of a parallel combination of bulk resistance and capacitance.

References

[1] S. Ozaki, Kei-Ichi Muto, H. Nagata, S. Adachi, J. Appl. Phys. 97 (2005) 043507.
[2] P. Babu, M.V. Reddy, N. Revathi, K.T.R. Reddy, J. Nano-Electron. Phys. 3 (2011) 85.
[3] J. Luengo, N.V. Joshi, Mater. Lett. 26 (1996) 47.
[4] J. Filipowicz, N. Romeo, L. Trricone, Solid State Commun. 38 (1981) 619.
[5] X. Sun, Y. He, J. Feng, J. Cryst. Growth 312 (2009) 48.
[6] Y. Ohtake, T. Okamoto, A. Yamada, M. Konagai, K. Saito, Sol. Energy Mater. Sol. Cells 49 (1997) 269.
[7] Y. Ohtake, S. Chaisitsak, A. Yamada, M. Konagai, Jpn. J. Appl. Phys. 37 (1998) 3220.
[8] M. Sugiyama, A. Kinoshita, A. Miyama, H. Nakanishi, S.F. Chichibu, J. Cryst. Growth 310 (2008) 794.
[9] S.P. Yadav, P.S. Shinde, K.Y. Rajpure, C.H. Bhosale, Sol. Energy Mater. Sol. Cells 92 (2008) 453.
[10] S.P. Yadav, P.S. Shinde, K.Y. Rajpure, C.H. Bhosale, J. Phys. Chem. Solids 69 (2008) 1747.
[11] S.H. Choe, Curr. Appl Phys. 9 (2009) 1.
[12] H.M. Zeyada, M.S. Aziz, A.S. Behairy, Physica B 404 (2009) 3957.
[13] H.M. Abdelmoneim, Indian J. Pure Appl. Phys. 48 (2010) 562.
[14] A. Hanumaion, T. Bhimosankaram, S.V. Suryanarayan, g. Kumar, Bull. Mater. Sci. 17 (1997) 405.
[15] M. JCPDS—International Centre for Diffraction Data, ICCD card No. 80-0424 (2000).
[16] T.S. Shafai, R.D. Gould, Thin Solid Films 516 (2007) 383.
[17] A.O. Abu-Hilal, A.M. Saleh, R.D. Gould, Mater. Chem. Phys. 94 (2005) 165.
[18] T.K. Vishnuvardhan, V.R. Kulkarni, C. Basavaraja, S.C. Raghavendra, Bull. Mater. Sci. 29 (1) (2006) 77.
[19] S.R. Elliott, Adv. Phys 36 (1987) 135.
[20] M.A. Ahmed, U. Seddik, N.G. Imam, World J. Condens. Matter Phys. 2 (2012) 66.
[21] I.G. Austin, N.F. Mott, Adv. Phys. 18 (1969) 41.

[22] M.A. Ahmed, N. Okasha, R.M. Kershi, J. Magn. Magn. Mater. 321 (2009) 3967.
[23] S.R. Elliott, Solid State Commun. 28 (1978) 939.
[24] V.K. Bahatnagar, K.L. Bhatiam, J. Non-Cryst. Solids 119 (1990) 214.
[25] A.E. Bekheet, Physica B 403 (2008) 4342.
[26] K.K. Srivaslava, A. Kumar, O.S. Panwar, K.N. Lakshminarayan, J. Non-Cryst. Solids 33 (1979) 205.
[27] M.A.M. Seyam, A.E. Bekheet, A. Elfalaky, Eur. Phys. J. Appl. Phys. 16 (2001) 99.
[28] J.C. Giuntini, J.V. Zancheha, J. Non-Cryst. Solids 34 (1982) 419.
[29] J.M. Stevels, The Electrical Properties of Glasses, Handbuch der Pysik 1975 p. 350.
[30] S.S. Fouad, A.E. Bekheet, A.M. Farid, Physica B 322 (2002) 163.
[31] F. Yakuphanoglu, I.S. Yahia, G. Barim, B.Filiz Senkal, Synth. Met. 160 (2010) 1718.
[32] M.P. Dasari, K. Sambasiva Rao, P. Murali Krishna, G.Gopala Krishna, Acta Phys. Pol. A 119 (2011) 387.
[33] P.S. Sahoo, A. Panigrahi, S.K. Patri, R.N.P. Choudhary, Mater. Sci.-Poland 28 (2010) 763.
[34] D.C. Sinclair, A.R. West, J. Appl. Phys. 66 (1989) 3850.
[35] B.P. Das, R.N.P. Choudhary, P.K. Mahapatra, Indian J. Eng. Mater. Sci. 15 (2008) 152.